

OPEN

Citation: *Cell Death and Disease* (2016) 7, e2374; doi:10.1038/cddis.2016.278

Official journal of the Cell Death Differentiation Association

www.nature.com/cddis

***BNC2* is a putative tumor suppressor gene in high-grade serous ovarian carcinoma and impacts cell survival after oxidative stress**

Laura Cesaratto^{1,9}, Eleonora Grisard^{1,9}, Michela Coan^{1,2}, Luigi Zandonà¹, Elena De Mattia³, Elena Poletto⁴, Erika Cecchin³, Fabio Puglisi^{4,5}, Vincenzo Canzonieri⁶, Maria Teresa Mucignat¹, Antonella Zucchetto⁷, Gabriele Stocco⁸, Alfonso Colombatti¹, Milena S Nicoloso^{*1} and Riccardo Spizzo^{*1}

Rs3814113 is the single-nucleotide polymorphism (SNP) showing the strongest association with high-grade serous ovarian carcinoma (HGSOC) incidence and is located in an intergenic region about 44 kb downstream of basonuclin 2 (*BNC2*) gene. Lifetime number of ovulations is associated with increased risk to develop HGSOC, probably because of cell damage of extrauterine Müllerian epithelium by ovulation-induced oxidative stress. However, the impact of low-penetrance HGSOC risk alleles (e.g. rs3814113) on the damage induced by oxidative stress remains unclear. Therefore, the purpose of this study was to investigate whether rs3814113 genetic interval regulates *BNC2* expression and whether *BNC2* expression levels impact on cell survival after oxidative stress. To do this, we analyzed gene expression levels of *BNC2* first in HGSOC data sets and then in an isogenic cell line that we engineered to carry a 5 kb deletion around rs3814113. Finally, we silenced *BNC2* and measured surviving cells after hydrogen peroxide (H₂O₂) treatment to simulate oxidative stress after ovulation. In this paper, we describe that *BNC2* expression levels are reduced in HGSOC samples compared with control samples, and that *BNC2* expression levels decrease following oxidative stress and ovulation *in vitro* and *in vivo*, respectively. Moreover, deletion of 5 kb surrounding rs3814113 decreases *BNC2* expression levels in an isogenic cell line, and silencing of *BNC2* expression levels increases cell survival after H₂O₂ treatment. Altogether, our findings suggest that the intergenic region located around rs3814113 regulates *BNC2* expression, which in turn affects cell survival after oxidative stress response. Indeed, HGSOC samples present lower *BNC2* expression levels that probably, in the initial phases of oncogenic transformation, conferred resistance to oxidative stress and ultimately reduced the clearance of cells with oxidative-induced damages.

Cell Death and Disease (2016) 7, e2374; doi:10.1038/cddis.2016.278; published online 22 September 2016

Epithelial ovarian cancer (EOC) is a relatively uncommon tumor accounting for ~2.6% of newly diagnosed tumors in 2015 in the United States; however, EOC is the fifth most common cause of cancer death in women in the United States and in the Western countries, and the first among gynecological tumors.¹ High-grade serous ovarian carcinoma (HGSOC) is the single largest group of EOC and the histotype that accounts for almost two-thirds of ovarian cancer deaths. HGSOC is typically diagnosed in postmenopausal age and at advanced clinical stages (III and IV), mainly owing to the lack of early symptoms and of affordable screening programs applicable to the general population.² For these reasons, it is

urgent to discover the key molecular events that predispose to and/or occur in the early phases of HGSOC oncogenic transformation, which are necessary for the development of effective screening tools, chemoprevention programs^{3,4} and eventually novel anticancer therapies.⁵

Recent reports elucidated novel details about the origin of HGSOC: studies from women carrying *BRCA1/2* mutations identified tubal intraepithelial carcinoma in the distal fimbriated end of the fallopian tube as the probable precursor lesion of HGSOC.⁶ This may also occur in the secondary Müllerian system locations (e.g. ovary and peritoneum) that, along with fallopian tube, belong to the extrauterine Müllerian epithelium.^{7,8}

¹Division of Experimental Oncology2, Department of Translational Research, Centro di Riferimento Oncologico (CRO Aviano), National Cancer Institute, Aviano, Italy;

²Department of Life and Reproduction Sciences, University of Verona, Verona, Italy; ³Division of Experimental and Clinical Pharmacology, Department of Translational Research Centro di Riferimento Oncologico (CRO Aviano), National Cancer Institute, Aviano, Italy; ⁴Department of Oncology, University Hospital of Udine, Udine, Italy;

⁵Department of Medical and Biological Sciences, University of Udine, Udine, Italy; ⁶Division of Pathology, Department of Translational Research, CRO Aviano National Cancer Institute, Aviano, Italy; ⁷Clinical and Experimental Onco-Hematology Unit, Centro di Riferimento Oncologico (CRO Aviano), National Cancer Institute, Aviano, Italy and ⁸Department of Life Sciences, University of Trieste, Trieste, Italy

*Corresponding author: R Spizzo or MS Nicoloso, Division of Experimental Oncology2, Department of Translational Research, Centro di Riferimento Oncologico (CRO Aviano), National Cancer Institute, Aviano 33081, Italy. Tel: +39 0434659820. Fax: +39 0434659428; E-mail: rspizzo@cro.it or mnicoloso@cro.it

⁹These authors contributed equally to this work.

Abbreviations: HGSOC, high-grade serous ovarian carcinoma; SNP, single-nucleotide polymorphism; *BNC2*, basonuclin 2; H₂O₂, hydrogen peroxide; EOC, epithelial ovarian cancer; TIC, tubal intraepithelial carcinoma; *BRCA1/2*, breast cancer; GWAS, genome-wide association studies; TSS, transcription starting point; *CNTLN*, centlein gene; LD, linkage disequilibrium; FTE, fallopian tube epithelium; H3K4me3, histone 3 lysine 4 tri-methylation; H3K27Ac, histone 3 lysine 27 acetylation; ChIP, chromatin immunoprecipitation; PBMC, peripheral blood mononuclear cell; CRISPR, clustered regularly interspaced short palindromic repeat; ROS, reactive oxygen species

Received 16.1.16; revised 04.7.16; accepted 29.7.16; Edited by A Oberst

In HGSOC, the most important risk factor is the occurrence of the disease in a first-degree relative;⁹ this excess of risk is because of both environmental (e.g. lifetime number of ovulations, body mass index and so on) and genetic factors. Concerning environmental factors, lifetime number of ovulations was one of the first to be described,¹⁰ and rodent models of repeated superovulation confirmed the insurgence of modifications resembling early transformation.^{11,12} The explanation of the association between lifetime number of ovulations and HGSOC incidence may reside in cell damage by ovulation-induced oxidative stress.^{11,13} Concerning genetic risk factors, which have the greatest impact, less than half of the excess of risk is due to *BRCA1/2* high penetrance mutations, whereas the remaining risk is probably because of low- to moderate-penetrance risk alleles.¹⁴ Low- to moderate-penetrance risk alleles (e.g. single-nucleotide polymorphism (SNP)) can be identified by genome-wide association studies (GWAS)¹⁵ and ultimately give novel molecular insights on tumor biology.^{16–18}

SNP rs3814113 has the strongest association with HGSOC incidence¹⁴ and is located in an intergenic region of human 9p22.2 locus, ~44 kb downstream from the transcription starting point (TSS) of basonuclein 2 (*BNC2*) gene and ~200 kb upstream from TSS of centlein (*CNTLN*) gene. *BNC2* transcribes a zinc-finger protein highly conserved during evolution,¹⁹ with about 200 transcript isoforms,²⁰ and *BNC2*-knockout (KO) mice die within 24 h after birth.²¹ Preliminary evidences pointed to *BNC2* as the coding transcript that could be responsible for the association between 9p22.2 locus and HGSOC: *BNC2* promoter is more frequently methylated in peripheral lymphomonocytes of EOC patients compared with healthy subjects,²² *BNC2* expression levels are reduced in EOC cell lines compared with primary human ovarian surface epithelial cell cultures,²³ and *BNC2* was described as a presumptive tumor suppressor gene in bladder, esophageal and glioblastoma tumors.^{24–26}

The impact of low-penetrance HGSOC risk alleles (e.g. rs3814113) on cell damage induced by oxidative stress remains unclear. For instance, acquired genetic modifications, which reduce cell death after oxidative stress, may offer fallopian serous epithelial cells the advantage to survive despite carrying genetic damages caused by oxidative stress exposure.¹² Therefore, the purpose of this study was to investigate whether rs3814113 genetic interval regulates *BNC2* expression and whether *BNC2* expression levels impact cell survival after oxidative stress. To do this, first we engineered an isogenic cell line to carry a 5 kb deletion around rs3814113 and measured *BNC2* levels; next, we silenced *BNC2* expression levels, and after hydrogen peroxide (H₂O₂) treatment, which simulates oxidative stress after ovulation,¹¹ we measured cell survival.

Results

***BNC2* is in linkage with rs3814113 and is a putative tumor suppressor in HGSOC.** To consolidate that *BNC2* is the principal actor of the association between human 9p22.2 locus and HGSOC incidence, we used two independent strategies. First, we searched for SNPs in linkage disequilibrium (LD) with rs3814113 by using SNAP bioinformatics

tool,²⁷ and we discovered that rs3814113 is correlated ($r^2 \geq 0.8$) to other 11 SNPs located within 6.8 kb upstream (Figure 1a and Supplementary Table 1). Yet, recombination rates suggested a larger haplotypic block, which includes the first exon and intron of *BNC2*, embracing one of *BNC2* promoters, and includes additional SNPs that correlated to rs3814113 with an $r^2 \geq 0.5$ (Figure 1a and Supplementary Table 1). Within the identified haplotypic block, rs3814113 was the only SNP present in the Illumina SNP-chromatin immunoprecipitation (ChIP) array used in the GWAS study that initially correlated 9p22.2 region with EOC predisposition.¹⁴

In the second strategy, we searched for genes within the 9p22.2 locus differentially expressed between tumor-free control and HGSOC samples. To do this, we interrogated the gene data set by Tone *et al.*,²⁸ which analyzed microdissected non-malignant fallopian tube epithelium (FTE) and HGSOC samples using a high-density Affymetrix gene expression array (Affymetrix Human Genome U133 Plus 2.0 Array, Santa Clara, CA, USA). We correlated signal intensity levels of microarray probes located within ± 4 Mb from rs3814113 (Supplementary Figure S1A) with the sample type (i.e. FTE or HGSOC samples), and we found that *BNC2* locus was the region with the greatest number of probes inversely correlated with HGSOC (i.e. lower signal intensity in HGSOC compared with non-malignant FTE samples) (Supplementary Figure S1B and Figure 1b). Instead, *CNTLN*, which is the closest gene downstream of rs3814113, was not differentially expressed between the groups (Figure 1b). We confirmed these results in a second publically available data set²⁹ (Figure 1c). Meanwhile, we collected at our Institute an original cohort of HGSOC and tumor-free control samples (fallopian tube and ovarian), in which we confirmed by quantitative real-time PCR (qRT-PCR) that *BNC2* expression was reduced in HGSOC (Figure 1d). Therefore, both LD and gene expression data analyses pointed to *BNC2* as the most likely candidate genetic element involved in HGSOC predisposition.

Next, we measured *BNC2* transcript expression in a panel of 16 EOC cell lines (Figure 2a). By grouping EOC cells into likely and unlikely HGSOC,³⁰ we did not observe any significant difference in *BNC2* expression levels between the two groups. In seven likely HGSOC cell lines, *BNC2* protein expression was proportional to mRNA expression and showed several isoforms between 100 and 150 kDa (Figure 2b); moreover, *BNC2* was localized exclusively in the NP40 nuclear insoluble fraction (Supplementary Figures S2A and B) in agreement with Vanhoutteghem and Djian.¹⁹ Interestingly, of the 12 EOC cell lines that we genotyped for rs3814113, all carried the T allele in homozygosis (data not shown), which is the allele associated with increased EOC predisposition in the general population,¹⁴ whereas according to dbSNP build 141,³¹ the expected frequency for rs3814113 in the general population is 58% for T and 42% for C.

According to Vanhoutteghem and Djian²⁰ and Ghanbari *et al.*,³² *BNC2* has several putative promoters and enhancers, which is also confirmed by the Encode project³³ (Supplementary Figure S3); however, histone marks enriched in promoters and enhancers (H3K4me3 and H3K27Ac, respectively) have never been described in HGSOC cell models. Therefore, we performed ChIP for these histone

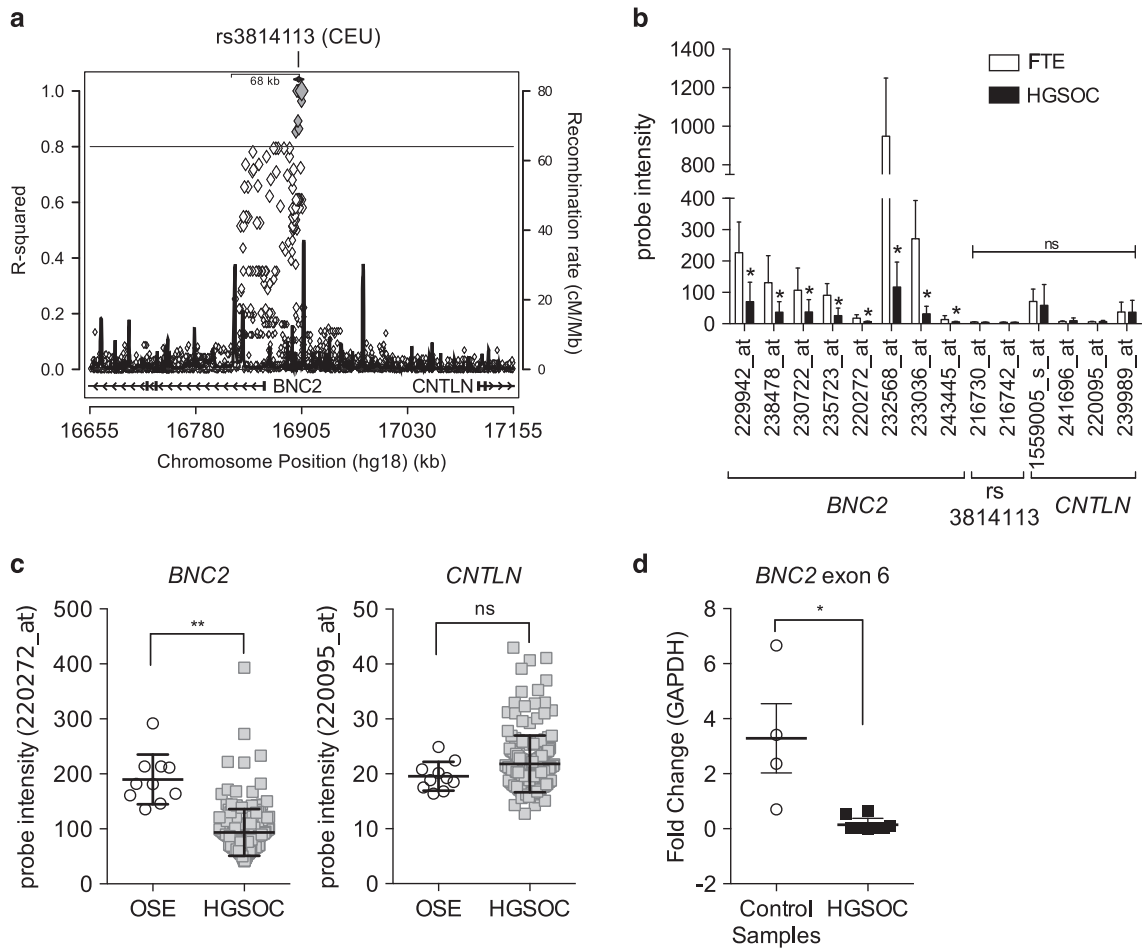


Figure 1 Rs3814113 at chromosome 9p22.2 is in linkage with *BNC2*, a putative tumor suppressor gene in HGSOc. **(a)** Regional LD plot generated using the SNP Annotation and Proxy Search web interface using rs3814113 as target SNP (<https://www.broadinstitute.org/mpg/snap/ldsearch.php>). The left-hand y axis shows values for r^2 (correlation coefficient, a measure of LD; 0.8 was set as threshold), whereas the right-hand y axis shows recombination rate values in centiMorgans (units of recombination) per million bases (cM/Mb). Diamond labels correspond to SNP (black diamond is rs3814113, gray filled diamonds represent SNPs with $r^2 \geq 0.8$ with rs3814113, empty filled diamonds have an $r^2 < 0.8$). Higher peaks of recombination rate indicate an association between rs3814113 and the end of *BNC2* genetic locus. **(b)** Analyses of gene expression for Affymetrix probes surrounding rs3814113 in the 9p22.2 locus from the GSE10971 data set. Affymetrix probes are indicated by a number followed by ‘_at’. Laser capture microdissected non-malignant distal FTE $n = 24$; HGSOc, $n = 13$. *BNC2*, intergenic region surrounding rs3814113, and *CNTLN* loci were represented in this array by 8, 2 and 4 probes, respectively. Bars are mean \pm S.E. **(c)** Analyses of *BNC2* and *CNTLN* expression in the GSE26712 data set. Non-malignant ovarian surface epithelium (OSE), $n = 10$; HGSOc, $n = 185$. In this Affymetrix array, *BNC2* and *CNTLN* were represented only by one probe (220272_at and 22095_at, respectively). Lines are mean \pm S.E. **(d)** qRT-PCR analysis of *BNC2* and *CNTLN* gene expression levels normalized by *GAPDH* in an original cohort of samples. Control samples = non-malignant ovarian and fallopian specimens, $n = 4$; HGSOc samples, $n = 10$. Scatter dot plot bars indicate mean \pm S.E. ** $P < 0.01$; * $P < 0.05$; ns, nonsignificant. *t*-Test assuming unequal variances was used for statistical analysis

marks in OV90, OVCAR4 and COV318 EOC cell lines. Consistent with *BNC2* mRNA and protein expression levels (Figures 2a and b), histone mark enrichment in candidate genetic regions was almost absent in OV90, intermediate in OVCAR4 and high in COV318 (Figure 2c). Moreover, in both COV318 and OVCAR4, the region labeled as *BNC2* Prom2 had the highest enrichment, in agreement with Ghanbari *et al.*³²

To sum up, these data indicate that the genomic region in LD ($r^2 \geq 0.5$) with rs3814113 includes one of the *BNC2* promoters and that *BNC2* is downregulated in HGSOc samples compared with non-malignant FTE samples.

A human genomic region including rs3814113 regulates *BNC2* expression. Interestingly, rs3814113 resides inside *AK024561* genomic locus, a putative non-coding RNA

transcript that was cloned in human adipose tissue according to GenBank records (Figure 3a). Two probes of the Affymetrix U133 Plus 2.0 Array hybridize to *AK024561* (i.e. 216730_at and 216742_at) (Supplementary Figure 3), but both show low expression signals and no difference between non-malignant FTE and HGSOc samples in Tone *et al.*²⁸ (Figure 1b and Supplementary Figure S1B). We evaluated expression levels of *AK024561* in a panel of 17 different non-malignant tissues, including peripheral blood mononuclear cells (PBMCs) collected from healthy donors, and in a panel of HGSOc samples, fallopian tube and ovary tumor-free samples. *AK024561* was strongly expressed only in the testis²⁰ and moderately expressed in the adrenal gland and skeletal muscle (Figure 3b). Only in 4 out of 10 HGSOc tumor samples, we could detect a faint band, whereas we did not

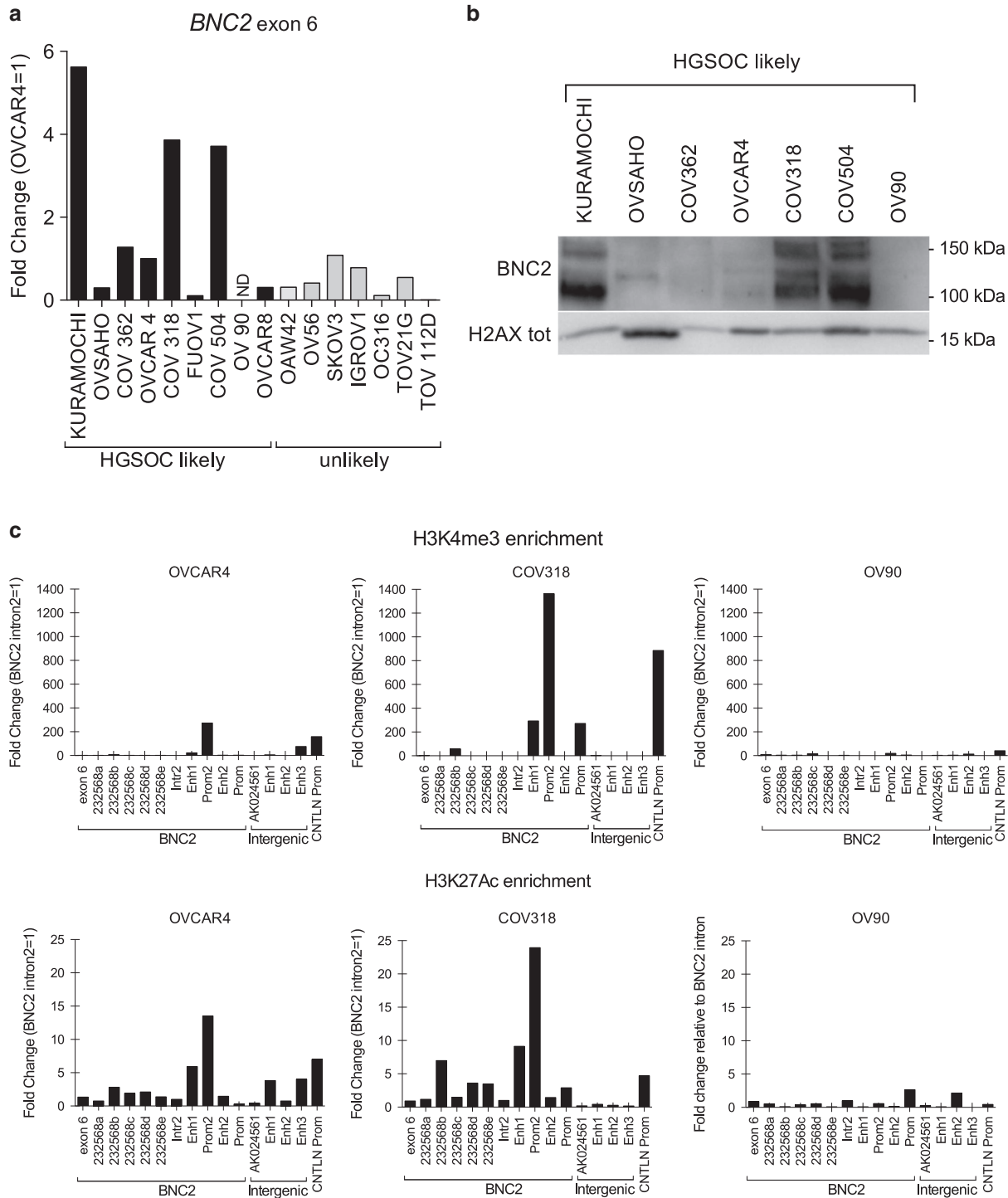


Figure 2 *BNC2* expression and genetic regulation. (a) qRT-PCR analysis of *BNC2* expression in a panel of 16 ovarian cancer cell lines, grouped in likely and unlikely HGSOE. (b) Western blot detection of *BNC2* shows several isoforms in NP40-insoluble protein extracts from seven likely HGSOE cell lines. H2AX total was used as loading control. (c) ChIP for histone mark enrichment (measured by qRT-PCR) in the putative promoter/enhancer genomic regions comprising *BNC2*, *CNTLN* and the intergenic region in between, according to UCSC (Supplementary Figure S3). H3K4me3 (top panels) and H3K27Ac (bottom panels) = histone H3 trimethylated on lysine 4 and acetylated on lysine 27, respectively. *BNC2* intron 2 (Intr 2) was set as 1

detect any band in the fallopian tube or ovarian healthy samples, except in one sample obtained from the round ligament (Figure 3b). We evaluated *AK024561* expression in several cell lines of mesodermal origin, the same origin of the

extrauterine Müllerian epithelium (COV318, COV504, COV362, OVCAR4, 293FT, JURKAT, MAVER, MEC, EHEB, HL60, RAJI, K562, SKUT-1, U2OS, HT1080, human mesenchymal stem cells, MET5A), but none showed any

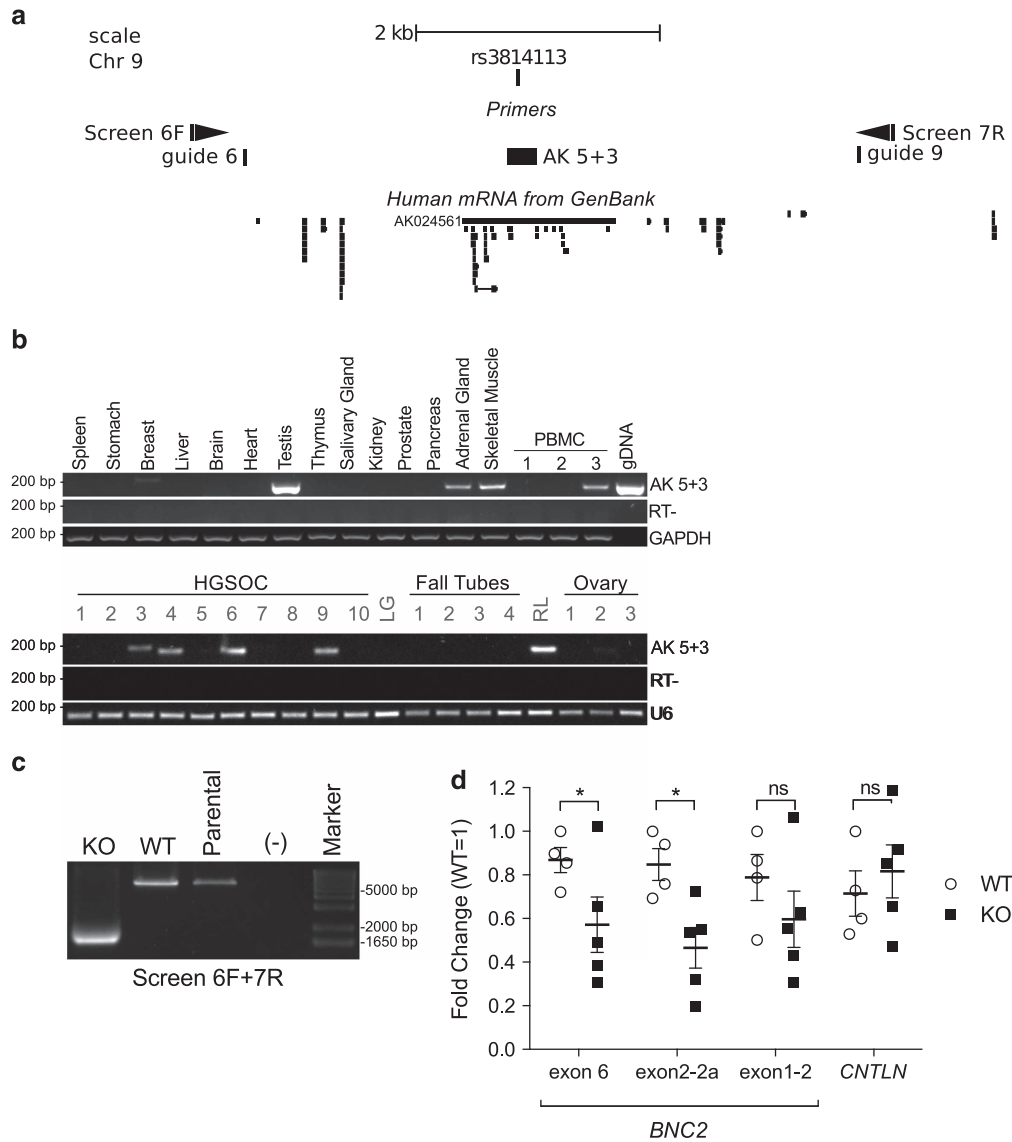


Figure 3 A human genomic region including rs3814113 regulates *BNC2* expression. (a) Genomic view of the 6.6 kb, surrounding rs3814113, with annotated human mRNAs from GenBank, according to UCSC genome browser. Positions for guides 6 and 9 (guide RNAs used for CRISPR (clustered regularly interspaced short palindromic repeat) deletion of the region), for Screen 6F and Screen 7F (primers used for PCR screening of KO), and for AK 5+3 (amplicon used to detect *AK024561* transcript) are indicated. (b) Agarose gel of PCR with AK 5+3 primers to detect *AK024561* in human samples: top panels, 14 normal human tissues and 3 PBMCs from healthy donors; bottom panels, 11 serous ovarian cancers (10 high grade, 1 low grade = LG) and 8 non-malignant control samples (4 fallopian tubes, 1 round ligament = RL, 3 ovaries). gDNA = genomic DNA used as PCR positive control; RT-PCR on non-retrotranscribed RNA, to exclude genomic contamination; *GAPDH* and *U6* = housekeeping genes used for normalization. (c) Representative agarose gel of PCR with Screen 6F+Screen 7R primer pair showing the deletion of the 5 kb region surrounding rs3814113. (d) qRT-PCR analysis of *BNC2* and *CNTLN* expression in 293FT KO cell clones. Points for WT and KO samples represent normalized expression data from four distinct WT and five distinct KO clones. The values for each clone are the average of two biologically independent experiments. Three distinct primer pairs (encompassing *BNC2*'s exon 1-2, exon 2-2a and exon 6) were used to detect *BNC2* expression levels. *t*-Test assuming unequal variances was used for statistical analysis. Scatter dot plot bars indicate mean \pm S.E. * $P < 0.05$. ns, nonsignificant

detectable expression levels except COV318, which had an extremely low signal (data not shown). Consistently, we did not observe histone mark enrichment in the intergenic regions including *AK024561* locus and nearby enhancers (intergenic enhancers 1, 2 and 3), except for a H3K27Ac enrichment in OVCAR4 intergenic enhancers 1 and 3 (Figure 2c).

To investigate whether *AK024561* locus may still regulate *BNC2* expression, we deleted 5 kb surrounding the SNP (between guide 6 and guide 9 in Figure 3a) using CRISPR-

Cas9 system.^{17,34} Unfortunately, we could not obtain KO cell clones in COV318, which is the only cell line, among the ones that we tested, that expressed *AK024561* (data not shown), because of the low efficiency of COV318 to grow as single-cell clones; therefore, we opted for 293FT because of very high efficiency of transfection and of single-cell clone recovery. We recovered five clones with homozygous deletion of the targeted region (KO clones) (Figure 3c and Supplementary Figure S4B), and we compared them with four wild-type (WT) clones, which had either point mutations in guide RNA target

sites ($n=2$) (guides 6 and 9 in Figure 3a) or no mutations ($n=2$) (sequences provided in the Supplementary Material). We measured *BNC2* and *CNTLN* transcript expression levels in WT and KO clones; given the multiplicity of *BNC2* isoforms,²⁰ we designed three qRT-PCR primer pairs that target exon boundary 1-2, 2-2a and exon 6²⁰ (Supplementary Figure S3). By these means, we observed that the deletion of the 5 kb region comprising rs3814113 almost halved expression levels of *BNC2* but not of *CNTLN* (Figure 3d). Unfortunately, 293FT expression levels of *BNC2* protein were almost undetectable and it was not possible to observe any difference between WT and KO clones. Of note, in 293FT cells, rs3814113 is heterozygous (C/T) and *AK024561* was never detected both in whole and nuclear RNA (data not shown).

Taken together, these findings indicate that the genetic region encompassing rs3814113 regulates *BNC2* but not *CNTLN* expression levels, and that this regulation does not depend on *AK024561* transcription.

Oxidative stress reduces *BNC2* expression *in vitro* and *in vivo*. The incessant ovulation model of EOC origin lies on the hypothesis that fallopian tubes and ovaries are exposed to increased levels of reactive oxygen species (ROS) during ovulation cycle, which reiterated over time may generate the soil for EOC insurgence.^{4,10,12} Therefore, to investigate whether *BNC2* may be involved in the incessant ovulation model, we evaluated *BNC2* expression levels following oxidative stress. To simulate postovulation environment, we treated OV90, COV318 and COV504 with increasing doses of H_2O_2 and evaluated *BNC2* levels at early and late time points, after 3 h and 24 h, respectively.³⁵ Effectiveness of H_2O_2 cell treatment was verified by phosphorylation of H2AX with no evident disparities among cell lines (Figure 4a and Supplementary Figure 5). While in OV90 *BNC2* levels remained undetectable even after H_2O_2 treatment (data not shown), in COV318 and COV504, we observed a dosage-dependent reduction of *BNC2* protein levels at 24 h after treatment, but not at earlier time points. To understand whether *BNC2* reduction occurred both at the transcriptional and protein level, we measured *BNC2* by qRT-PCR and found that, 5 h following H_2O_2 exposure, *BNC2* transcript levels were already halved, suggesting a regulation of *BNC2* at the transcriptional/mRNA level rather than at the protein stability level (Figure 4b). To address deeper the molecular

mechanism by which *BNC2* is regulated in an oxidative stress condition, we investigated the role of epigenetic modifications in *BNC2* expression at different time points after H_2O_2 exposure. To do this, we performed a time-course experiment in COV318 treated with 0.06 mM of H_2O_2 , which is the lowest dosage at which we previously observed a reduction of *BNC2* protein expression levels, and we confirmed that *BNC2* expression decreases both at mRNA and protein levels (Figures 4c and d). As *BNC2* promoter contains three CpG islands (Supplementary Figure S3) and *BNC2* promoter methylation has been previously found associated with EOC,²² we analyzed methylation status of CpG island 141 (chr9:16870124–16872020 hg19) and CpG island 21 (chr9:16828936–16829169 hg19) and did not observe any methylation both in untreated and treated cells (data not shown). Concomitantly, we evaluated activating and repressing histone modifications (H3K4me3 and H3K27me3, respectively) in the same time-course experiment. Unexpectedly, activating H3K4me3 modification increased at earlier time points and eventually decreased at 24 h (Figure 4e), whereas we did not find any enrichment of repressing H3K27me3 modification (data not shown). We also wondered whether *BNC2* repression persisted longer than 24 h after H_2O_2 exposure; indeed, we found *BNC2* downregulation both at mRNA and protein levels lasting up to 1 week post-treatment (Figures 4f and g), likely due to a decrease of activating H3K4me3 enrichment and an increase of suppressing H3K27me3 in *BNC2* promoters and enhancers (Figure 4h). Enrichment of H3K27me3 modification in H_2O_2 -treated COV318 cells was similar to OV90, which constitutively do not express *BNC2* (Figure 4h). According to our results, decrease of *BNC2* expression after H_2O_2 exposure is not due to methylation and histone modifications at early time points, whereas at later time points, histone modification is involved in *BNC2* transcription repression.

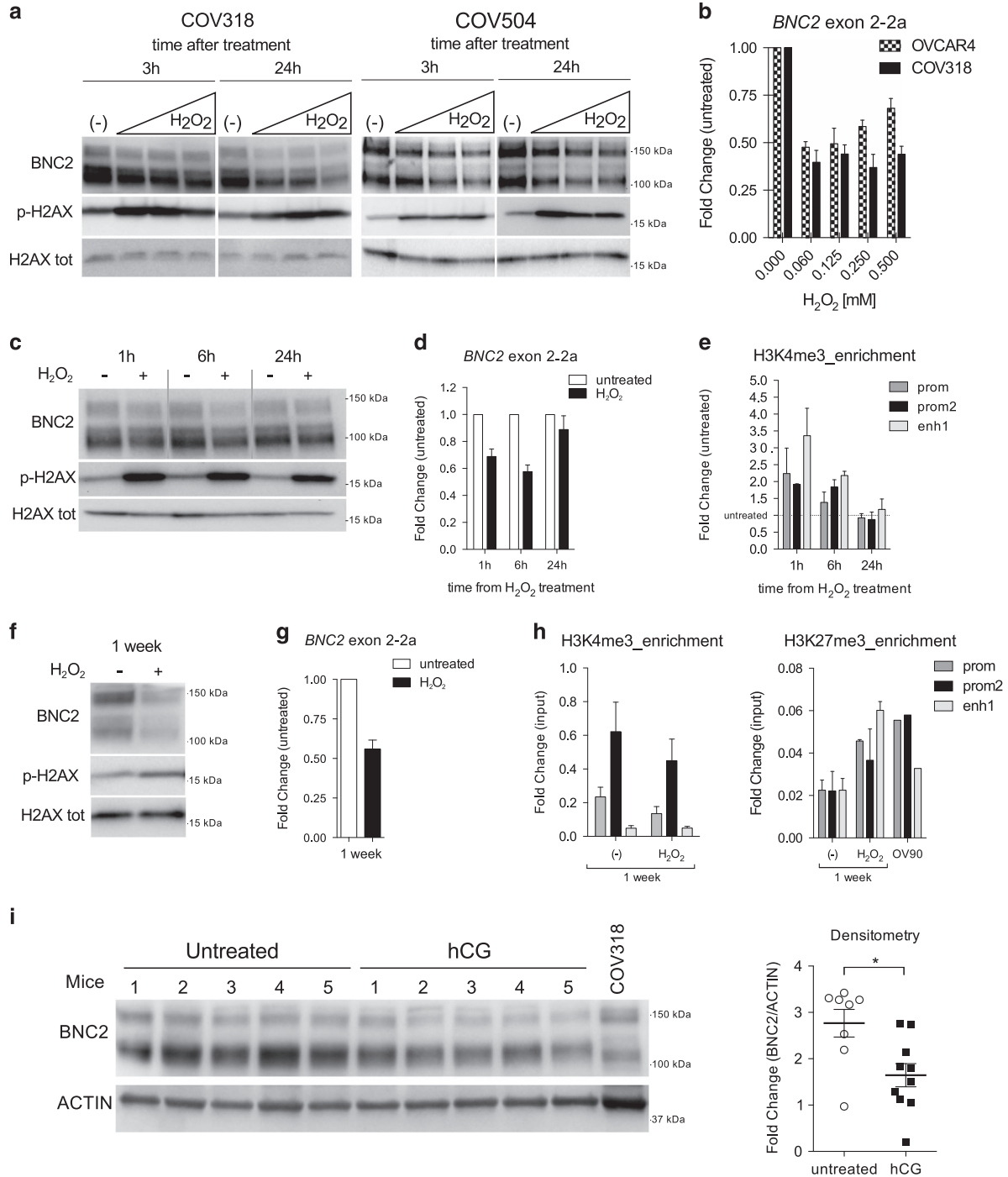
To study the effect of ovulation on *BNC2* expression levels *in vivo*, we induced superovulation in prepubertal mice and measured *BNC2* protein levels in murine oviducts. In this model, *BNC2* displayed several protein isoforms similarly to COV318, and its protein expression levels decreased in ovulated mice compared with control mice (Figure 4i).

To sum up, these evidences suggest that *BNC2* expression levels decrease both *in vitro* and *in vivo* after oxidative stress or ovulation, respectively.

Figure 4 Oxidative stress reduces *BNC2* expression *in vitro* and *in vivo*. (a) Western blot detection of *BNC2* protein levels in NP40-insoluble extracts from COV318 and COV504 cells treated with increasing amounts of H_2O_2 (0.06, 0.125 and 0.25 mM) at 3 or 24 h post-treatment. Total H2AX was used as loading control. Phospho-H2AX (pH2AX) was detected to check effectiveness of H_2O_2 treatment. (b) qRT-PCR analysis of *BNC2* expression in COV318 and OVCAR4 at 5 h after H_2O_2 treatment. Bars indicate mean \pm S.E. from two independent experiments. (c) Western blot detection of *BNC2* protein levels in NP40-insoluble extracts from COV318 cells treated with 0.06 mM H_2O_2 and collected 1, 6 and 24 h post-treatment. Total H2AX was used as loading control. pH2AX was detected to check effectiveness of H_2O_2 treatment. (d) qRT-PCR analysis of *BNC2* expression in COV318 at 1, 6 and 24 h after 0.06 mM H_2O_2 treatment. Bars indicate mean \pm S.E. from two independent experiments. (e) ChIP for H3K4me3 enrichment (measured by qRT-PCR) of three regulatory elements of *BNC2* locus in COV318 treated with 0.06 mM H_2O_2 at different time points. Bars indicate mean \pm S.E. from two independent experiments. (f) Western blot detection of *BNC2* protein levels in NP40-insoluble extracts from COV318 cells treated with 0.06 mM H_2O_2 and collected 1 week post-treatment. Total H2AX was used as loading control. pH2AX was detected to check effectiveness of H_2O_2 treatment. (g) qRT-PCR analysis of *BNC2* expression in COV318 at 1 week after 0.06 mM H_2O_2 treatment. Bars indicate mean \pm S.E. from two independent experiments. (h) ChIP for H3K4me3 enrichment (left panel) and H3K27me3 enrichment (right panel) (measured by qRT-PCR) of three regulatory elements of *BNC2* locus in COV318 at 1 week after 0.06 mM H_2O_2 treatment. Bars indicate mean \pm S.E. from two independent experiments. (i) Left panel: Western blot detection of *BNC2* protein levels in NP40-insoluble extracts from prepubertal mice oviducts treated or not with hCG 16 h earlier. COV318 was used as positive control for *BNC2* expression. Right panel: Densitometric analysis of *BNC2* western blot bands in oviducts from hCG treated ($n=10$) and untreated ($n=10$) prepubertal mice as described above. Scatter dot plot bars indicate mean \pm S.E. from two independent experiments, including the one presented in the left panel. * $P < 0.05$

BNC2 silencing increases ovarian cell survival following H₂O₂ treatment. Next, we argued whether BNC2 levels affect cell survival after oxidative stress. To this aim, we treated OV90 (no BNC2 expression), OVCAR4 (intermediate BNC2 expression) and COV318 (high BNC2 expression) (Figure 2b) with increasing doses of H₂O₂; 24 h after treatment, we measured surviving cells by MTT assay. Interestingly, we observed that OV90 cells are resistant to H₂O₂

treatment (>80% alive); at the same dosages, OVCAR4 and COV318 showed a degree of H₂O₂ sensitivity that was inversely correlated with BNC2 expression levels (Figure 5a). With this observation in mind, we silenced BNC2 levels by shRNA in three different BNC2-expressing HGSOE cell lines and in BNC2-null OV90 cell line. We tested five short hairpins spanning different regions of *BNC2* (Supplementary Figure S3), and used the ones with a strong and intermediate



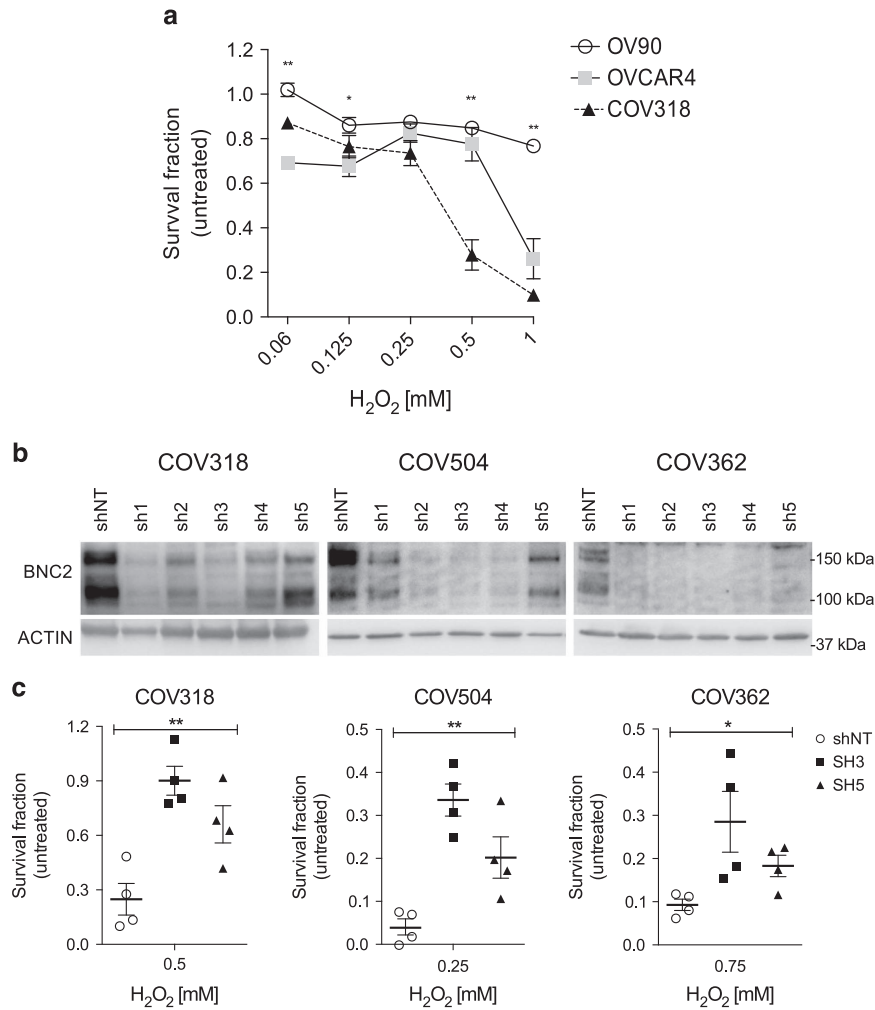


Figure 5 *BNC2* silencing increases ovarian cancer cell survival following H₂O₂ treatment. (a) MTT viability, expressed as fold change compared with untreated cells (= 1), of OV90, OVCAR4 and COV318 cells 24 h following H₂O₂ treatment. ***P* < 0.01, **P* < 0.05 using *t*-test assuming unequal variances. Points in graph represent average ± S.E. of three independent biological replicates. (b) Western blot detection of *BNC2* protein levels in NP40-insoluble extracts from COV318, COV362 and COV504 expressing five different short hairpins (sh) targeting *BNC2*. shNT = sh non-target, negative control. (c) Scatter dot plot resume MTT viability experiments, expressed as fold change compared with untreated cells (= 1), of COV318, COV362 and COV504 silenced (sh3 and sh5) or not (shNT) for *BNC2* 24 h following H₂O₂ treatment. ***P* < 0.01, **P* < 0.05 using one-way analysis of variance (ANOVA) test. Scatter dot plot bars indicate mean ± S.E. of four replicates (two independent biological experiments performed in duplicate). Results from different H₂O₂ treatments for each cell line are shown: COV318 (0.5 mM), COV362 (0.75 mM) and COV504 (0.25 mM)

silencing ability (sh3 and sh5) for further experiments (Figure 5b and Supplementary Figure S6A). When we treated *BNC2*-silenced cells with H₂O₂, we observed that silenced cells were more resistant to H₂O₂ compared with control cells in three HGSOc cell lines (Figure 5c); this effect was not recapitulated in OV90 (Supplementary Figure 6B), which are null for *BNC2*, indicating that the phenotype that we described was *BNC2*-specific. Cells silenced with sh5, which always displayed the smallest *BNC2* reduction, were also the ones with the smallest increase in cell survival, implying that the effect that we observed was dependent on *BNC2* expression levels.

In conclusion, these evidences indicate that low *BNC2* expression levels have a protective role in response to H₂O₂, which is in line with reduced expression levels of *BNC2* in HGSOc compared with control samples (Figures 1b–d).

Discussion

Our study showed that the first intron and exon of *BNC2* and one of its promoters are in linkage with rs3814113, and that *BNC2* expression levels were reduced in HGSOc samples compared with control samples. Moreover, we observed that deletion of 5 kb surrounding rs3814113 decreased *BNC2* expression levels in an isogenic cell line and, finally, that silencing of *BNC2* expression levels increased HGSOc cell survival after H₂O₂ treatment.

Altogether, our findings give new insights about the mechanism at the basis of HGSOc and 9p22.2 association,¹⁴ and in particular they suggest that the intergenic region located around rs3814113 regulates *BNC2* expression, which in turn affects cell survival after oxidative stress response. Indeed, HGSOc samples present lower *BNC2* expression levels that,

in the initial phases of oncogenic transformation, may confer resistance to oxidative stress and ultimately reduce the clearance of cells with ROS-induced damages.

So far, few groups have published results regarding the role of *BNC2* in cancer, but all suggested a putative tumor suppressor function of *BNC2*,^{24–26} in agreement with our findings. Ramus *et al.*³⁶ reported that rs3814113 minor allele (C) is also associated to a lower risk of EOC in *BRCA1/2*-mutated populations. When we analyzed the gene expression data set from Tone *et al.*,²⁸ which contains both *BRCA1/2* WT and mutant control samples, we did not observe any difference in *BNC2* expression levels between the two groups (data not shown). Ultimately, these evidences may suggest that *BNC2* locus and *BRCA1/2* loci are two independent risk factors in EOC onset.

Our study presents some limitations: for instance, (1) we used cell lines derived from HGSOC and not cell lines derived from normal tissues (e.g. normal fallopian tubes); nevertheless, we confirmed our *in vitro* findings in the normal oviducts obtained from a mouse model of superovulation. (2) We did not investigate in our cell model the allele-specific impact of rs3814113 on *BNC2* expression, as we expected that it would have taken a GWAS-size clones to observe any effect. Instead, we took advantage of an isogenic cell line knocked out for 5 kb interval surrounding rs3814113 to obtain a stronger effect. Despite having found a link between rs3814113 genomic region and *BNC2* expression, we cannot exclude that other genetic elements that are located in the haplotypic block of rs3814113 participate in *BNC2* regulation. (3) Finally, even though we described that silencing of *BNC2* expression affects survival after H₂O₂ treatment, despite our attempts, we could not generate cells overexpressing *BNC2* to rescue silencing experiments and we did not dissect in greater detail the molecular mechanism at the basis of this phenotype. Precisely, our results on *BNC2* localization in agreement with¹⁹ suggest that *BNC2* is localized in the nucleus more firmly compared with transcription factors and is a putative chromatin-modulating protein; therefore, ChIP-seq would be a good approach to study *BNC2* binding regions.

EOC and breast cancer share some common risk factors (e.g. *BRCA1/2* status); therefore, it might be expected that *BNC2* has a role also in breast cancer onset. We are not aware of *BNC2* expression levels in normal and tumor breast samples; however, there is no report of any association between rs3814113 and breast cancer risk, in both the general population¹⁵ and *BRCA1/2* mutant carriers,³⁶ ultimately suggesting that *BNC2* is not involved in breast cancer.

According to our results, *BNC2* seems to be a good candidate to develop new molecular tools to select healthy subjects with increased risk of EOC. Despite having demonstrated that the 5 kb region around rs3814113 regulates *BNC2* expression, it is unlikely that we can use rs3814113 genotyping as an indicator of *BNC2* expression¹⁴ and novel strategies should be undertaken. At the same time, we showed that *BNC2* silencing affects cell survival after oxidative stress, which suggests that modulating *BNC2* levels pharmacologically may be an intriguing strategy to reduce the excess of EOC risk in selected populations (e.g. *BRCA1/2* mutation carriers). Ultimately, if we consider that the discovery of high

penetrance risk alleles (*BRCA1/2* mutations) not only helped to identify subjects at higher risk but it was also helpful to select EOC patients benefiting the most from poly(ADP-ribose) polymerase inhibitors,⁵ the same scenario may also be true for *BNC2*. Hence, understanding how to target *BNC2* and/or the associated stress response pathway could lead to the development of alternative therapeutic approaches for patients with HGSOC.

Materials and Methods

Cell lines, cell cultures, lentiviral transduction and transfections.

Cell lines used in this work are listed in Supplementary Table 2, which includes cell type, source and culture media. No antibiotics were routinely used for cell culture. Cells have been authenticated in 2012 by BMR Genomics (Padova, Italy) according to Cell ID System (Promega, Madison, WI, USA) and using Genemapper ID version 3.2.1, to identify DNA STR profiles. Cells were expanded and have been used only for a short number of passages after authentication. Cell lines were maintained at 37 °C under 5% CO₂ in humidified incubators and routinely tested using MycoAlert Detection Kit (Lonza, Cologne, Germany) for mycoplasma contamination. Only mycoplasma-negative cells were used for experiments.

BNC2-silenced ovarian cancer cell lines were generated by lentiviral transduction. Briefly, 293FT cells were co-transfected with pLKO.1 puro vectors encoding for either human *BNC2*-shRNAs (sh1_TRCN0000108177, sh2_TRCN0000327841 sh3_TRCN0000108179, sh4_TRCN0000108175, sh5_TRCN0000108176, MISSION shRNAs from Sigma-Aldrich (St. Louis, MO, USA)) or non-target shRNA control (SHC016; Sigma-Aldrich), together with ViraPower Packaging Mix (pLP1, pLP2 and pLP/VSV-G) (Invitrogen, Thermo Fisher Scientific, Eugene, OR, USA). Viral supernatants were collected 72 h later and transducing units per ml were determined by limiting dilution titration in HCT116 cells. An MOI of ~5 was used for transducing ovarian cancer cells. After 5 days of selection with puromycin, *BNC2*-silenced cells were immediately used for *in vitro* experiments, protein and RNA extraction. Polybrene (Sigma-Aldrich) at a final concentration of 8 µg/ml was used to increase transduction efficiency.

Cell transfections were performed using Lipofectamine 2000 reagent (Invitrogen, Thermo Fisher Scientific) according to the manufacturer's instructions.

CRISPR-Cas9 system. KO of *AK024561* in 293FT cells was generated by CRISPR-Cas9 system, according to Ran *et al.*,³⁴ using two guide RNAs (guides 6 and 9; Supplementary Table 3) that delimit a region of 5 kb surrounding the *AK024561* non-coding transcript (Figure 3a). To this end, guide RNAs were cloned into pSpCas9(BB)-2A-GFP (PX458) vector (cat. no. 48138; Addgene, Cambridge, MA, USA) and transfected into cells. To evaluate guide RNA-directed Cas9 cutting efficiency, genomic DNA was extracted using Genra Puregene Cell Kit (Qiagen Sciences, Germantown, MD, USA), according to the manufacturer's instructions, and was subjected to Surveyor Assay using Surveyor Mutation Detection Kit (IDT Integrated DNA Technologies, Leuven, Belgium), as per the manufacturer's instructions (Supplementary Figure 4A).

The 293FT CRISPR-modified cell clones were grown following GFP single-cell sorting by FACS, then genomic DNA was extracted and clones were screened by PCR, using two primers, *AK024561* 5+3 and Screen 6F+7R (Figure 3a and Supplementary Table 3), which for KO clones were expected to yield no product and a 1.6 kb fragment, respectively (Figure 3c and Supplementary Figure S4). Genetic deletion was confirmed by direct Sanger sequencing, using BigDye Terminator v.3.1 Cycle Sequencing Kit (Applied Biosystems, Foster City, CA, USA). Sequences of all the clones that we used are reported in Supplementary Material.

Cell treatments. H₂O₂ treatment was performed as follows: cells plated 24 h earlier in a 6- or 12-well format were exposed for 1 h to H₂O₂ (0–4 mM range) in serum-free medium. After two washes with PBS, H₂O₂ containing medium was removed and replaced with complete medium. Cell viability was assayed 24 h later by MTT staining (M2003; Sigma-Aldrich). MTT stock solution was added to cells at a final concentration of 0.28 mg/ml and incubated for 1 h at 37 °C. Supernatant was then discarded and cells were air-dried. Reduced MTT, measure of cellular metabolic activity and index of cell viability was dissolved by adding 1 or 2 ml of DMSO, depending on plate format. Two hundred microliters of DMSO were transferred to a 96-well and absorbance was measured at 570 nm with Infinite M1000 Microplate Reader (Tecan, Männedorf, Switzerland).

Western blotting. To obtain protein extracts, cells were incubated for 20 min on ice in lysis buffer (0.5% NP40, 50 mM HEPES, 250 mM NaCl, 5 mM EDTA, 0.5 mM EGTA, 1 μ M DTT), containing Protease Inhibitors (Complete; Roche, Mannheim, Germany) and Phosphatase Inhibitor Cocktail 1 and 2 (P2850 and P5726; Sigma-Aldrich), vortexing every 5 min. Cell lysates were clarified by centrifugation at a maximum speed for 10 min (NP40-soluble fraction). Cell pellet was then suspended in SDS lysis buffer (4% SDS, 100 mM Tris-HCl (pH 6.8), 20% glycerol) and boiled at 95 °C for 10 min (NP40-insoluble fraction, containing chromatin-bound proteins, such as BNC2). Protein concentration of the NP40-soluble fraction was quantified using the Protein Assay Dye Reagent Concentrate (Bio-Rad, Hercules, CA, USA), whereas the concentration of the NP40-insoluble fraction was empirically derived from its corresponding soluble fraction.

For immunoblotting analysis, ~40 μ g of proteins were separated using 4–20% SDS-PAGE Criterion TGX Stain-Free Precast Gels (Bio-Rad) and transferred to PVDF membranes (Bio-Rad). Membranes were blocked with 5% non-fat dried milk in TBS-0.1% Tween-20, and incubated overnight with the following antibodies: BNC2 (HPA018525; Sigma-Aldrich), ACTIN (cat. no. A2066; Sigma-Aldrich), histone H2AX (cat. no. 2595; Cell Signaling, Danvers, MA, USA) and phospho-histone H2AX (Ser139) (20E3) (cat. no. 2577; Cell Signaling). Incubation with ECL rabbit IgG, HRP-linked whole antibody (GE Healthcare Lifesciences, Little Chalfont, UK) was performed at room temperature for 1 h at a dilution of 1 : 3000. According to signal intensity, either ECL Western Blotting Detection Reagents RPN 2106 (GE Healthcare) or Luminata Forte Western HRP Substrate (Merck Millipore, Darmstadt, Germany) were used for secondary antibody detection using Chemidoc MP Imager (Bio-Rad). Bands were analyzed and quantified using Image Lab v.5.2 (Bio-Rad).

ChIP assay. Before harvesting, 3×10^7 cells were crosslinked with 1% (v/v) of formaldehyde in complete culture medium for 10 min at room temperature and then quenched with 125 mM glycine. Cell pellets were washed two times with ice-cold PBS and then lysed in 1 ml of ChIP lysis buffer (1% SDS, 50 mM Tris-HCl (pH 8.1), 10 mM EDTA), completed with Protease Inhibitors (Complete; Roche) and Phosphatase Inhibitor Cocktail 1 (P5726; Sigma-Aldrich). Lysates were sonicated with an ultrasonic homogenizer Sonopuls 3200 (Bandelin, Berlin, Germany) for 12 cycles (30 s ON+60 s OFF) and clarified by centrifugation. DNA fragment size was checked in a 2% agarose gel with a 100 bp DNA marker. Fifty micrograms of protein extract, diluted 10-fold in ChIP dilution buffer (0.01% SDS, 1.1% Triton X-100, 1.2 mM EDTA, 16.7 mM Tris-HCl (pH 8.1) and 167 mM NaCl), were incubated, for 2 h with rotating at 4 °C, with 2 μ g of the following specific ChIP grade antibodies: anti-histone H3-acetyl K27, H3 tri-methyl K4 (cat. no. ab4729, ab8580; Abcam, Cambridge, UK) and H3 tri-methyl K27 (cat. no. 9733; Cell Signaling). Immunoprecipitation was performed by using Protein A Sepharose 4 Fast Flow (GE Healthcare) overnight at 4 °C. After several washes of the IP samples (in low salt, in high salt and in LiCl wash buffers), the elution was performed incubating in 1% SDS and 100 mM NaHCO₃ for 45 min with rotation at room temperature. To reverse crosslinking, supernatants were collected and incubated at 65 °C overnight with the addition of NaCl, 200 mM final concentration. Samples were subjected to DNA extraction using Genra Puregene Cell Kit (Qiagen) according to the manufacturer's instructions. DNA levels for the 9p22.2 regions of interest were quantified by qRT-PCR using specific primers (Supplementary Table 3).

RNA extraction, cDNA synthesis and qRT-PCR. RNA was extracted using the Isol-RNA lysis reagent (5 Prime, Hamburg, Germany) according to protocol instructions. Extraction was followed by PCA (phenol: chloroform: isoamyl alcohol 25 : 24 : 1; Sigma-Aldrich) purification that reduces salt contamination and by DNase digestion (Turbo-Dnase, Ambion, Thermo Fisher Scientific). RNA quality was assessed using agarose gel electrophoresis after RNA exposure to 70 °C for 5 min. cDNA was synthesized from 1 μ g of RNA using the AMV Reverse Transcriptase (Promega) with random primers (Promega). cDNA was diluted 10 times and used for qRT-PCR using iQ SYBR Green Supermix (Bio-Rad) with the appropriate primers (Supplementary Table 3). qRT-PCR reactions were carried out either in a 96-well optical reaction plates using Two-Color Real-Time PCR Detection System MyiQ2 (Biorad) or in 384-well optical reaction plates using Applied Biosystems 7900HT Fast Real-Time PCR System (Thermo Fisher Scientific), according to manufacturer's protocol. The $2^{-\Delta\Delta Ct}$ method was used to calculate the relative abundance of RNA genes, measuring *GAPDH* expression as housekeeping control.

Primers used in this work were designed using Primer 3 Plus,³⁷ purchased from Sigma-Aldrich and are listed in Supplementary Table 3.

In vivo experiments. Prepubertal FVB female mice (between 3 and 5 weeks of age) were stimulated with 5 μ IU of serum gonadotropin (Folligon, Schering-Plough Animal Health, Upper Hutt, Wellington, New Zealand) and 48 h later with 5 μ IU of human chorionic gonadotropin (Chorulon, MSD Animal Health, Madison, NJ, USA) or with placebo (0.9% NaCl) by intraperitoneal injection. After 16 h, mice were humanely culled, assessed for ovulation and oviducts were collected. NP40-soluble and -insoluble proteins were extracted from oviducts, as described above. Animal experiments were reviewed and approved by the CRO Aviano's Institutional Animal Care and Use Committee and were conducted according to committee's guidelines.

Patient samples. Samples were obtained at CRO Aviano, National Cancer Institute (Aviano, Italy) according to Cervo *et al.*³⁸ after informed consent forms were signed, through CRO-Biobank facility. Scientific use of biological material was approved by CRO Aviano's Ethics Committee and Internal Review Board. Control ovarian and fallopian tube samples were collected from women undergoing annexectomy for diseases other than ovarian and fallopian tubes cancers, whereas HGSOC specimens were collected from ovarian cancer patients undergoing first-line cytoreductive surgery (by laparoscopy or laparotomy). CRO Aviano's Pathology Unit performed sample pathologic evaluation as part of standard routine on fresh-frozen specimens and confirmed a tumor percentage >70%.

Statistical and gene expression analysis. Graphs presented in figures were obtained using the GraphPad Prism v.6.0d software (La Jolla, CA, USA) and statistical analysis were carried out using the JMP v.9.0.1 software (Carry, NC, USA). Data were examined using the two-tailed Student's *t*-test assuming unequal variances or one-way ANOVA test when we compared more than two groups at once. Differences were considered significant at $P < 0.05$ and $P < 0.01$ and labeled accordingly (* or **, respectively).

Data sets used for gene expression analysis include Gene Expression Omnibus IDs: GSE10971²⁸ and GSE26712.²⁹ For each set, gene signal values were background corrected, normalized by the quantile method and reported as log₂-transformed values, as implemented in the *rma* function of the Affy R package.

Conflict of Interest

The authors declare no conflict of interest.

Acknowledgements. We thank Cytometry Core Facility (Clinical and Experimental Onco-Hematology Unit, CRO Aviano) for helpful support in the cell sorting experiments. We are grateful to Dr. Gustavo Baldassarre, to Fatima Mectha Grigoriou and Riccardo Fodde for insightful scientific discussions. This publication is in partial fulfillment of the requirements for a PhD in Biosciences and Biotechnology – Curriculum in Cell Biology, University of Padova of Eleonora Grisard. This work was supported by grants from Italian Ministry of Health (GR-2010-2319387) and Talents Marie Curie Actions/Regione Friuli Venezia Giulia (Grant Agreement No. 245574) to RS, from Italian Association for Cancer Research (AIRC, MFAG No. 13589) and Marie Curie Actions (CIG No. 303877) to MSN and from 5x1000 to CRO Aviano.

1. National Cancer Institute. *PDQ Ovarian Cancer Treatment*. National Cancer Institute: Bethesda, MD. Available at: <http://www.cancer.gov/research/progress/snapshots/ovarian> (last accessed January 2016).
2. National Cancer Institute. *A Snapshot of Ovarian Cancer*. National Cancer Institute: Bethesda, MD. (last accessed January 2016).
3. Rothwell PM, Fowkes FG, Belch JF, Ogawa H, Warlow CP, Meade TW. Effect of daily aspirin on long-term risk of death due to cancer: analysis of individual patient data from randomised trials. *Lancet* 2011; **377**: 31–41.
4. Kotsopoulos J, Lubinski J, Gronwald J, Cybulski C, Demsky R, Neuhausen SL *et al.* Factors influencing ovulation and the risk of ovarian cancer in BRCA1 and BRCA2 mutation carriers. *Int J Cancer* 2015; **137**: 1136–1146.
5. Fong PC, Boss DS, Yap TA, Tutt A, Wu P, Mergui-Roelvink M *et al.* Inhibition of poly(ADP-ribose) polymerase in tumors from BRCA mutation carriers. *N Engl J Med* 2009; **361**: 123–134.
6. Bowtell DD, Bohm S, Ahmed AA, Aspuria PJ, Bast RC Jr, Beral V *et al.* Rethinking ovarian cancer II: reducing mortality from high-grade serous ovarian cancer. *Nat Rev Cancer* 2015; **15**: 668–679.
7. Ng A, Barker N. Ovary and fimbrial stem cells: biology, niche and cancer origins. *Nat Rev Mol Cell Biol* 2015; **16**: 625–638.
8. Dubeau L. The cell of origin of ovarian epithelial tumours. *Lancet Oncol* 2008; **9**: 1191–1197.
9. National Cancer Institute. *PDQ Ovarian Cancer Treatment*. National Cancer Institute: Bethesda, MD. Available at: <http://www.cancer.gov/types/ovarian/hp/ovarian-epithelial-treatment-pdq> (last accessed January 2016).

10. Fathalla MF. Incessant ovulation – a factor in ovarian neoplasia? *Lancet* 1971; **2**: 163.
11. King SM, Hilliard TS, Wu LY, Jaffe RC, Fazleabas AT, Burdette JE. The impact of ovulation on fallopian tube epithelial cells: evaluating three hypotheses connecting ovulation and serous ovarian cancer. *Endocr Relat Cancer* 2011; **18**: 627–642.
12. Stewart SL, Querec TD, Ochman AR, Gruver BN, Bao R, Babb JS et al. Characterization of a carcinogenesis rat model of ovarian preneoplasia and neoplasia. *Cancer Res* 2004; **64**: 8177–8183.
13. Lau A, Kollara A St., John E, Tone AA, Virtanen C, Greenblatt EM et al. Altered expression of inflammation-associated genes in oviductal cells following follicular fluid exposure: implications for ovarian carcinogenesis. *Exp Biol Med* 2014; **239**: 24–32.
14. Song H, Ramus SJ, Tyrer J, Bolton KL, Gentry-Maharaj A, Wozniak E et al. A genome-wide association study identifies a new ovarian cancer susceptibility locus on 9p22.2. *Nat Genet* 2009; **41**: 996–1000.
15. Welter D, MacArthur J, Morales J, Burdett T, Hall P, Junkins H et al. The NHGRI GWAS catalog, a curated resource of SNP-trait associations. *Nucleic Acids Res* 2014; **42**: D1001–D1006.
16. Spisak S, Lawrenson K, Fu Y, Csabai I, Cottman RT, Seo JH et al. CAUSEL: an epigenome- and genome-editing pipeline for establishing function of noncoding GWAS variants. *Nat Med* 2015; **21**: 1357–1363.
17. Sur IK, Hallikas O, Vaharautio A, Yan J, Turunen M, Enge M et al. Mice lacking a Myc enhancer that includes human SNP rs6983267 are resistant to intestinal tumors. *Science* 2012; **338**: 1360–1363.
18. Ling H, Spizzo R, Atlasi Y, Nicoloso M, Shimizu M, Redis RS et al. CCAT2, a novel noncoding RNA mapping to 8q24, underlies metastatic progression and chromosomal instability in colon cancer. *Genome Res* 2013; **23**: 1446–1461.
19. Vanhoutteghem A, Djian P. Basonuclins 1 and 2, whose genes share a common origin, are proteins with widely different properties and functions. *Proc Natl Acad Sci USA* 2006; **103**: 12423–12428.
20. Vanhoutteghem A, Djian P. The human basonuclin 2 gene has the potential to generate nearly 90,000 mRNA isoforms encoding over 2000 different proteins. *Genomics* 2007; **89**: 44–58.
21. Vanhoutteghem A, Maciejewski-Duval A, Bouche C, Delhomme B, Herve F, Daubigny F et al. Basonuclin 2 has a function in the multiplication of embryonic craniofacial mesenchymal cells and is orthologous to disco proteins. *Proc Natl Acad Sci USA* 2009; **106**: 14432–14437.
22. Winham SJ, Armasu SM, Cicek MS, Larson MC, Cunningham JM, Kalli KR et al. Genome-wide investigation of regional blood-based DNA methylation adjusted for complete blood counts implicates BNC2 in ovarian cancer. *Genet Epidemiol* 2014; **38**: 457–466.
23. Goode EL, Chenevix-Trench G, Song H, Ramus SJ, Notaridou M, Lawrenson K et al. A genome-wide association study identifies susceptibility loci for ovarian cancer at 2q31 and 8q24. *Nat Genet* 2010; **42**: 874–879.
24. Akagi T, Ito T, Kato M, Jin Z, Cheng Y, Kan T et al. Chromosomal abnormalities and novel disease-related regions in progression from Barrett's esophagus to esophageal adenocarcinoma. *Int J Cancer* 2009; **125**: 2349–2359.
25. Nord H, Hartmann C, Andersson R, Menzel U, Pfeifer S, Piotrowski A et al. Characterization of novel and complex genomic aberrations in glioblastoma using a 32 K BAC array. *Neuro-oncology* 2009; **11**: 803–818.
26. Beothe T, Zubakov D, Kovacs G. Homozygous losses detected by array comparative genomic hybridization in multiplex urothelial carcinomas of the bladder. *Cancer Genet* 2015; **208**: 434–440.
27. Johnson AD, Handsaker RE, Pulit SL, Nizzari MM, O'Donnell CJ, de Bakker PI. SNAP: a web-based tool for identification and annotation of proxy SNPs using HapMap. *Bioinformatics* 2008; **24**: 2938–2939.
28. Tone AA, Begley H, Sharma M, Murphy J, Rosen B, Brown TJ et al. Gene expression profiles of luteal phase fallopian tube epithelium from BRCA mutation carriers resemble high-grade serous carcinoma. *Clin Cancer Res* 2008; **14**: 4067–4078.
29. Bonome T, Levine DA, Shih J, Randonovich M, Pise-Masison CA, Bogomolnii F et al. A gene signature predicting for survival in suboptimally debulked patients with ovarian cancer. *Cancer Res* 2008; **68**: 5478–5486.
30. Domcke S, Sinha R, Levine DA, Sander C, Schultz N. Evaluating cell lines as tumour models by comparison of genomic profiles. *Nat Commun* 2013; **4**: 2126.
31. Sherry ST, Ward MH, Kholodov M, Baker J, Phan L, Smigielski EM et al. dbSNP: the NCBI database of genetic variation. *Nucleic Acids Res* 2001; **29**: 308–311.
32. Ghanbari M, de Vries PS, de Looper H, Peters MJ, Schurmann C, Yaghootkar H et al. A genetic variant in the seed region of miR-4513 shows pleiotropic effects on lipid and glucose homeostasis, blood pressure, and coronary artery disease. *Hum Mutat* 2014; **35**: 1524–1531.
33. Landt SG, Marinov GK, Kundaje A, Kheradpour P, Pauli F, Batzoglou S et al. ChIP-seq guidelines and practices of the ENCODE and modENCODE consortia. *Genome Res* 2012; **22**: 1813–1831.
34. Ran FA, Hsu PD, Wright J, Agarwala V, Scott DA, Zhang F. Genome engineering using the CRISPR-Cas9 system. *Nat Protocols* 2013; **8**: 2281–2308.
35. King SM, Burdette JE. Evaluating the progenitor cells of ovarian cancer: analysis of current animal models. *BMB Rep* 2011; **44**: 435–445.
36. Ramus SJ, Kartsonaki C, Gayther SA, Pharoah PD, Sinilnikova OM, Beesley J et al. Genetic variation at 9p22.2 and ovarian cancer risk for BRCA1 and BRCA2 mutation carriers. *J Natl Cancer Inst* 2011; **103**: 105–116.
37. Untergasser A, Nijveen H, Rao X, Bisseling T, Geurts R, Leunissen JA. Primer3Plus, an enhanced web interface to Primer3. *Nucleic Acids Res* 2007; **35**: W71–W74.
38. Cervo S, Rovina J, Talamini R, Perin T, Canzonieri V, De Paoli P et al. An effective multisource informed consent procedure for research and clinical practice: an observational study of patient understanding and awareness of their roles as research stakeholders in a cancer biobank. *BMC Med Ethics* 2013; **14**: 30.



Cell Death and Disease is an open-access journal published by **Nature Publishing Group**. This work is licensed under a **Creative Commons Attribution 4.0 International License**. The images or other third party material in this article are included in the article's Creative Commons license, unless indicated otherwise in the credit line; if the material is not included under the Creative Commons license, users will need to obtain permission from the license holder to reproduce the material. To view a copy of this license, visit <http://creativecommons.org/licenses/by/4.0/>

© The Author(s) 2016

Supplementary Information accompanies this paper on Cell Death and Disease website (<http://www.nature.com/cddis>)